# On the Numerical Integration
# of the Schrödinger Equation:
# Numerical Tests

R. Guardiola

*Departamento de Física Nuclear,*
*Universidad de Granada, Granada, Spain*

AND

J. Ros

*Departamento de Física Teórica,*
*Universidad de Granada, Granada, Spain*

The various numerical methods obtained in a preceding work in the finite-difference scheme are compared among themselves and against the exact solutions of some simple, exactly soluble potentials. The tests strongly favour the limiting method, the discretized plane-wave method. A discussion of the results in the continuous spectrum is also presented.

## 1. Introduction

In a previous work [1], hereafter referred to as I, we have studied in a unified framework all numerical methods for the integration of the Schrödinger equation (and, in general, for the integration of the homogeneous Sturm–Liouville problem) in the finite-difference scheme at constant step. We may briefly summarize our results by saying that all numerical methods of common use are generated through the various Padé approximants to the Taylor expansion of the operator $D^2 = d^2/dr^2$ in terms of the central second-difference operator $\delta^2$ with step $h$, defined as $\delta^2 f(r) = f(r - h) - 2f(r) + f(r + h)$. The numerical methods are classified by two numbers, $[N/M]$, corresponding to the degree in $\delta^2$ of the polynomials of the numerator and denominator of the Padé approximant, respectively. The order of the error, i.e., the first power of $h$ neglected, is given by $2(N + M + 1)$.

These various $[N/M]$ methods have received special names in the literature: the family $[N/0]$ corresponds to the so-called Taylor-$(2N + 2)$ methods, the family $[1/N]$ corresponds to the Numerov-$(2N + 4)$ methods and the family $[N/N]$ with $N \geqslant 2$ corresponds to the extended Numerov-$(4N + 2)$ methods.

390

Another result of I, and the most important in our opinion, was the fact that the referred Taylor expansion is convergent and can be easily summed up, giving rise to our discretized plane-wave (PW) method. All these methods have a point in common, namely, that the required values of the potential are $V(nh)$, i.e., the values at a mesh of constant step $h$, with $n$ varying from 1 to some maximum value $N_p$.

Certainly, all numerical formalisms call for numerical tests, and this is the main goal of the present work. We should say, however, before presenting the various tests, that there are no *magic* procedures for the numerical solution of any problem. In other words, none of the methods described in I should be straightforwardly applied to determine the bound states and phase shifts of a given potential, and some questions, such as the appropriate value of the number of points $N_p$, the optimal value of the step (i.e., the largest value compatible with the desired error), and the correct sampling (i.e., the appropriate change of variables) are questions which cannot be answered a priori and which may require a large amount of numerical trials and/or a detailed study of the properties of the potential under study.

The paper is organized as follows: Section 2 is devoted to the analysis of the results of the numerical integration, with a particular (and, it is hoped, novel) emphasis on the solutions in the continuum. In Section 3 we present the study of four analytically soluble potentials which behave differently enough so as to include most of the situations of practical interest (long tails, a core at short distances, weakly bound states, etc.,). Finally, the conclusions, results, and prospectives of this work are presented in Section 4.

All numerical work has been carried out with a "personal computer" based on the 6502 microprocessor chip. This is already a "result" of our work which we would like to stress here: the microcomputers are very slow systems (some 100 to 10,000 times slower than the usual scientific computers) and this means that the PW method may be very efficiently coded and run in a large system in very short times. The computer program is very simple: it is only necessary to construct the various matrices and proceed to their diagonalization. For the diagonalization, we have used the algorithm Nb. 384 of the CACM(2), which has proven to be both quick and stable. The precision of our calculations is of 40 bits per word, approximately 9 digits.

## 2. The Discrete and the Continuous Spectrum in Global-Matrix Methods

The matrix methods for the integration of the Schrödinger equation are grounded in the simple boundary conditions that the solution is zero at $r = 0$ and at a given $R_{max}$ (in the case of one-dimensional problems these conditions are changed so that the wave function is null at some $R_{min}$ and $R_{max}$ approaching $\pm\infty$). Once $R_{max}$ has been decided one has to assume a value for the number of points $N_p$, the corresponding step being $h = R_{max}/(N_p + 1)$, and the solution of the differential equation is converted into the diagonalization of a real symmetric matrix. According

to I, the matrix to be diagonalized has a simple form in momentum space. The kinetic energy part is built up with the help of the matrix representation of $\delta^2$, namely,

$$[\delta^2]_{p,q} = -\delta_{pq} \, 4 \sin^2 \frac{p\pi}{2(N_p + 1)}, \tag{1}$$

and the corresponding formulae for the second derivatives of each $[N/M]$ approximation (see I, Eq. (9)). The resulting matrix for the kinetic energy then has a simple diagonal form. In the case of the PW method the form of the kinetic energy is still simpler,

$$\left[ -\frac{d^2}{dr^2} \right]_{p,q} = \left( \frac{p\pi}{h(N_p + 1)} \right)^2 \delta_{pq}. \tag{2}$$

To this matrix one has to add the matrix corresponding to the potential which in this representation is given by

$$[V]_{p,q} = \frac{2}{N_p + 1} \sum_{s=1}^{N_p} \sin \frac{sp\pi}{N_p + 1} \sin \frac{sq\pi}{N_q + 1} \, V(sh) \tag{3}$$

and proceed to the diagonalization. We stress that in the case of the PW method it is not necessary to compute the momentum representation of the potential: in configuration space the PW for of the kinetic energy is very simple (see I, Eq. (32)), and the potential is diagonal with values $V_{pp} = V(ph)$.

After the solution of the matrix-eigenvalue problem there result $N_p$ non-degenerate real solutions which may be classified according to the number of nodes: no nodes for the lowest solution, one node for the next, and so on (the nodes at $r = 0$ and $r = R_{max}$ are not included in this counting). In the case of a confining potential, $V(r) \to \infty$ at $r \to \infty$, all these solutions should correspond to bound states. On the contrary, for the potentials of most common interest, mainly attractive at short or medium distances and going to zero at infinity, only those solutions with negative energy do correspond to bound states.

We have found only a few indirect references to the meaning of the solutions in the continuum arising from the global-matrix formulation of the Schrödinger equation, these solutions being termed as spurious. There are reasons for using that adjective, as far as there is not quantization in the continuum, the Schrödinger equation having solutions at every value of the energy. The boundary condition imposed at $R_{max}$ however, leads to an energy quantization: among the continuum of solutions for positive energy only those which are null at $r = R_{max}$ appear in the solution of the matrix-eigenvalue problem. On the other hand, this fact is sufficient to determine the phase shifts. Let us assume that there are $N_b$ bound states; the $n$th solution of positive energy has $N_b + n - 1$ nodes, plus the nodes at $r = 0$ and $R_{max}$. Then, the phase of this solution has had a change of $(N_b + n)\pi$ in the interval $(0, R_{max})$. If the energy is $E_n$, then the phase shift is obtained from the simple equation

$$E_n^{1/2} R_{max} + \delta = (N_b + n)\pi. \tag{4}$$

In this form, the absolute phase shift (and not modulus $\pi$) is obtained. The disadvantage of the method is that we do not obtain the phase shift at a predetermined energy, but instead the phase shift at the discrete set of energy values resulting from the diagonalization. Certainly, a small change in $R_{max}$ would imply a small change in the eigenvalues of the continuum (and should not change the negative eigenvalues at all if $R_{max}$ is large enough) in such a form that we may obtain the phase shifts at other sets of energy values. Note that Eq. (4) must be appropriately changed for angular momentum states other than zero.

A byproduct of the above discussion is that it offers a simple and intuitive picture of Levinson's theorem.

## 3. NUMERICAL EXAMPLES

The first case we have considered is that of the harmonic oscillator potential. The radial equation in this case is given by

$$\left(-\frac{d^2}{dr^2} + r^2 + \frac{l(l+1)}{r^2}\right)\Psi = E\Psi$$ (6)

in units such that $m = 1/2$, $\hbar = 1$, and $\omega = 2$, and the energy levels are given by

$$E = 2(2n + l + \tfrac{3}{2}), \qquad n = 0, 1, 2,\dots.$$ (7)

TABLE I

The First Six States of the Harmonic Oscillator Potential in $s$-Waves

| PW | 3.0000000 | 6.9999996 | 11.000000 | 15.000000 | 19.000000 | 23.000000 |
|---|---|---|---|---|---|---|
| (1/0) | 2.9538719 | 6.7650318 | 10.414268 | 13.888676 | 17.171248 | 20.238154 |
| (2/0) | 2.9970840 | 6.9743809 | 10.908256 | 14.776006 | 18.554757 | 22.219834 |
| (3/0) | 2.9997143 | 6.9961201 | 10.940344 | 14.940334 | 18.858118 | 22.713925 |
| (4/0) | 2.9999629 | 6.9992803 | 10.995225 | 14.981533 | 18.947882 | 22.879739 |
| (1/1) | 2.9988169 | 6.9891644 | 10.959372 | 14.896240 | 18.784728 | 22.607236 |
| (1/2) | 2.9999081 | 6.9986883 | 10.993094 | 14.977290 | 18.942731 | 22.877854 |
| (1/3) | 2.9999894 | 6.9997808 | 10.998452 | 14.993604 | 18.980700 | 22.952426 |
| (2/2) | 2.9999973 | 6.9999411 | 10.999553 | 14.997991 | 18.993406 | 22.982372 |
| (3/3) | 3.0000000 | 6.9999991 | 10.999993 | 14.999949 | 18.999743 | 22.999000 |

The results for $l = 0$ corresponding to the various methods considered are shown in Table I, for a mesh of 20 points and $R_{max} = 8$. The results of this table are clearly impressive with regard to the PW and the [3/3] methods. We should also mention that the first of the levels computed with the PW method, which differs appreciably from the exact value, is the level $n = 12$, its energy being 51.0113 against the exact value 51. There is in Table I a remarkable characteristic, also present in the other calculations, which is the convergence of the subfamilies of methods toward the PW results with increasing $N + M$. Furthermore, among the methods with the same order of error, like [4/0], [1/3], and [2/2], the best is the diagonal Padé form.

In Table II we show the error in the calculation of the g.s. for the various methods and for several number of points. It is an appealing fact that the PW method is monotonic, whereas the other methods may give results higher or lower than the exact value. This point must be considered when comparing the goodness of the various numerical methods: actually, the error may be very small for some value of $N_p$, as in the case of the [4/0] method at $N_p = 6$, but this does not mean that the result is good, because we may still be far from the stability against the number of points, as in the mentioned case.

Finally, we show in Table III a large number of levels of the harmonic oscillator computed with the PW method with 20 points and for several values of the angular momentum. The most remarkable result of the table is that the odd angular momentum levels are not as well determined as the even angular momentum levels. Moreover, within the set of odd levels, the higher the angular momentum the better the result. We shall analyze these facts in the next section.

TABLE II

Absolute Error in the Calculation of the g.s. of the Harmonic Oscillator with $R_{max} = 8$

| N. POINTS | 4 | 6 | 8 | 10 | 12 |
|---|---|---|---|---|---|
| PW | 0.586 | 0.038 | 0.0006 | 3.E-6 | 2.E-7 |
| (1/0) | 0.321 | -0.309 | -0.267 | -0.177 | -0.125 |
| (2/0) | 0.469 | -0.094 | -0.074 | -0.036 | -0.019 |
| (3/0) | 0.521 | -0.028 | -0.029 | -0.011 | -0.004 |
| (4/0) | 0.545 | -0.0004 | -0.014 | -0.004 | -0.001 |
| (1/1) | 0.512 | -0.040 | -0.039 | -0.017 | -0.009 |
| (1/2) | 0.548 | 0.002 | -0.013 | -0.004 | -0.002 |
| (1/3) | 0.563 | 0.017 | -0.006 | -0.002 | -0.0005 |
| (2/2) | 0.573 | 0.027 | -0.003 | -0.0006 | -0.0002 |
| (3/3) | 0.583 | 0.035 | 0.0001 | -0.0001 | -6.E-6 |

TABLE III

Energy Levels of the Harmonic Oscillator Potential Computed with the PW Method for Various Angular Moments, $R_{max} = 8$

| EXACT | L=0 | 1 | 2 | 3 | 4 | 5 |
|-------|-----|---|---|---|---|---|
| 3 | 3.000000 | | | | | |
| 5 | | 4.988812 | | | | |
| 7 | 7.000000 | | 7.000000 | | | |
| 9 | | 8.969818 | | 8.999981 | | |
| 11 | 11.000000 | | 11.000000 | | 11.000000 | |
| 13 | | 12.942740 | | 12.999905 | | 13.000000 |
| 15 | 15.000000 | | 15.000000 | | 15.000000 | |
| 17 | | 16.906426 | | 16.999703 | | 16.999998 |
| 19 | 19.000000 | | 19.000000 | | 19.000000 | |
| 21 | | 20.859113 | | 20.999257 | | 20.999995 |
| 23 | 23.000000 | | 22.999999 | | 23.000000 | |
| 25 | | 24.798393 | | 24.998375 | | 24.999983 |
| 27 | 27.000001 | | 27.000001 | | 27.000000 | |
| 29 | | 28.721208 | | 28.996740 | | 28.999948 |
| 31 | 31.000000 | | 31.000003 | | 31.000000 | |
| 33 | | 32.623896 | | 32.993816 | | 32.999860 |
| 35 | 34.999998 | | 35.000001 | | 35.000001 | |
| 37 | | 36.502535 | | 36.988687 | | 36.999642 |
| 39 | 39.000007 | | 39.000006 | | 39.000005 | |

*Note.* The first column includes the exact results.

The second case considered is the Hylleraas potential (3), which gives rise to the reduced equation

$$\left(-\frac{d^2}{dr^2} - VCh^{-2}r/R\right)\Psi = E\Psi. \tag{8}$$

The bound states are classified by the number $n$ in the range

$$n = 1, 2, \cdots < ((1 + 4R^2V)^{1/2} + 1)/4 \tag{9}$$

their energy being [4]

$$E_n = -R^{-2}\{(R^2V + \tfrac{1}{4})^{1/2} - 2n + \tfrac{1}{2}\}^2. \tag{10}$$

TABLE IV

The Energy of the Three Bound States of the Hylleraas Potential

|          | G. S.       | 1ST        | 2ND        |
| -------- | ----------- | ---------- | ---------- |
| EXACT    | 18.201156   | 5.136031   | 0.070906   |
| PW       | 18.201089   | 5.135686   | 0.062169   |
| (1/0)    | 18.729237   | 6.347958   | 0.489896   |
| (2/0)    | 18.283581   | 5.370231   | 0.121502   |
| (3/0)    | 18.221797   | 5.205347   | 0.079488   |
| (4/0)    | 18.208030   | 5.162051 · | 0.068897   |
| (1/1)    | 18.239104   | 5.246514   | 0.088817   |
| (1/2)    | 18.209323   | 5.164479   | 0.069288   |
| (1/3)    | 18.203754   | 5.146225   | 0.064881   |
| (2/2)    | 18.202072   | 5.139781   | 0.063243   |
| (3,3)    | 18.201167   | 5.136074   | 0.062279   |

The only relevant combination in this formula is the product $R^2 V$. Then we have taken $R = 1$ and $V = 33$ so that the potential has three bound states with energies $-18.201156$, $-5.136031$, and $-0.070906$. The reason for the selection of these parameters is the presence of a weakly bound state, because the levels near the edge of the well are rather hard to determine numerically. The results corresponding to this potential are shown in Table IV, for $R_{max} = 9$ and $N_p = 30$. An important remark on this potential is the necessity of using a large value of $R_{max}$ in order to bind the third state: actually for the calculation with $N_p = 20$ and $R_{max} = 6$ which has almost the same step, the reported calculation gives the same results for the g.s. and the first excited level, but the second excited level is off by one order of magnitude. The results corresponding to this level in Table IV are still far from the stability region and should not be used for comparison among the various methods.

With regard to the other two levels the PW method gives much better results than the others, with the exception of the [3/3]. In that method the results are sometimes better than those of the PW by a slight amount.

In the Hylleraas potential we also study the s-wave phase shifts. The values for $R_{max} = 6$ and 20 mesh points are shown in Fig. 1 as a function of the energy and compared with the theoretical results obtained from the S-matrix [5]. Given that the theoretical results are modulus $\pi$, the phase shifts have been adjusted so that they go to zero at high energy, and adding a sufficient number of $\pi$ so as to have a smooth behaviour with the energy. From the figure we see that agreement with the exact results improves when $N + M$ increases, as in the previous situations. Furthermore,
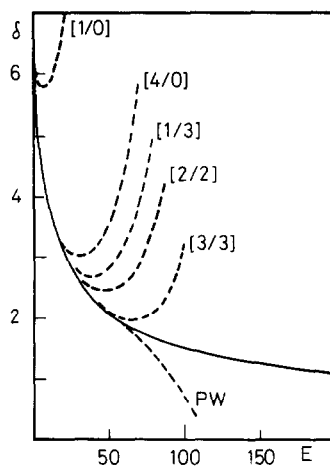
Fig. 1. Comparison of the exact phase shifts (—) with the computed values for the Hylleraas potential. The phase shift is measured in radians and the energy in natural units. $R_{max} = 6$ and $N_p = 20$.

the quality of the PW results is much higher than in any of the other methods. A calculation with 40 points at the same value of $R_{max}$ with the PW method gives phase shifts in very good agreement up to energies of 350 in our units.

A third case of interest, which has been the subject of much controversy [6, 7] in the last decade, is the Morse [8] potential. This potential is currently used to describe the vibrational levels of diatomic molecules, and the controversy originated from sizable differences between the calculations of several groups. The Morse potential in reduced form gives rise to the eigenvalue equation

$$\left(-\frac{d^2}{dr^2} + V\{1 - \exp 2b(r - R)/R\}^2\right)\Psi = E\Psi, \tag{11}$$

where $R$ is the equilibrium separation of the atoms. This potential supports a set of bound states labelled by a quantum number $n$ in the range

$$n = 1, 2, \cdots < RV^{1/2}/2b + \tfrac{1}{2} \tag{12}$$

the energies being approximately [4]

$$E_n = -(4b^2/R^2)(n - \tfrac{1}{2} - (RV^{1/2}/2b))^2 \tag{13}$$

when the conditions $RV^{1/2} \exp(2b)/b \gg RV^{1/2} \gg 1$ are satisfied. We have used the values [6] $V = 31,250$ and $b/R = 2^{1/2}$. This does not completely specify the potential, the equilibrium distance $R$ still being a free parameter. However, $R$ does not enter in the values of the energy, provided the above inequalities are satisfied (only the combination $R/b$ is relevant). A usual value for $R$ is 1.5 Å.

An intrinsic problem related to this potential comes from the strong repulsion at short distances: as far as the relevant combination appearing in finite-differences integration methods is $h^2 V$, there results the necessity of choosing a small value of the step to maintain the stability criterion $h^2 V \ll 1$ in the region close to the origin, and this means that one must use a very large number of points. An important reduction is reached by observing that the wave function should be very small in that region and suggests the convenience of moving the boundary condition from $r = 0$ to some $r = R_s$. This movement of the boundary condition is related to the irrelevance of $R$, within some limits, with respect to the energy: this new boundary condition is equivalent to a shift to the left of the whole potential, i.e., to change $R$ by $R - R_s$. A further observation helps in setting the numerical procedure, namely, the fact that the Morse potential behaves very much like a harmonic oscillator potential of frequency $\omega^2 = 16b^2 V/R^2$. From the point of view of global-matrix methods the above comments mean that to appropriately state the problem one has to impose the boundary conditions at some $R_{max}$ and $R_s$ symmetrically placed around the minimum of the well. With these facts in mind we have carried out the calculation of the lower levels of this potential by using $R - R_s = R_{max} - R = 0.36$ and with a mesh of odd number of points. The results corresponding to the PW method with 45 points are shown in Table V, compared with the values given by Eq. (13).

Our results are impressively good, and they compare very well (and are sometimes better) with the results obtained by specialized methods like Rayleigh–Ritz–Galerkin

TABLE V

Energy Levels of the Morse Potential

| N | EXACT | PW |
|---|-------|-----|
| 1 | 498 | 498.000 |
| 2 | 1482 | 1482.000 |
| 3 | 2450 | 2450.000 |
| 4 | 3402 | 3402.000 |
| 5 | 4338 | 4338.001 |
| 6 | 5258 | 5258.000 |
| 7 | 6162 | 6162.000 |
| 8 | 7050 | 7050.000 |
| 9 | 7922 | 7922.004 |
| 10 | 8778 | 8778.050 |
| 11 | 9618 | 9618.487 |

*Note.* The exact values are also included.

with the harmonic oscillator basis [7] or the sine basis [7, 9]. The main advantage of our method is that we do not require analytic integrations.

The final example considered is the exponential potential, the radial equation being

$$\left(-\frac{d^2}{dr^2} - V \exp(-r)\right) \Psi = E\Psi. \tag{14}$$

The bound levels of this potential may be determined by solving the trascendent equation [10]

$$J_{2\sqrt{E}}(2\sqrt{V}) = 0. \tag{15}$$

With $V = 20.25$ the potential has three bound levels with energies $-6.74726$, $-1.47543$, and $-0.01241$. We have devoted most of our computational work to this potential, because the behaviour of the numerical methods in this case is not easy to understand. In Table VI we report the error of the g.s. energy for a constant value of $R_{\max} = 10$ and for various values of the number of points of the mesh. In the table we observe that, with the exception of the simple Taylor-4 method, the results are surprisingly better for the a priori-worse methods, and the worst results correspond to our favourite PW method. The situation is analogous for the first excited level. With regard to the second excited level, no reliable results are obtained for this value of $R_{\max}$. Actually, we must go to $R_{\max} = 30$ and use a very large value of $N_p$ to bind this level with any of the methods. Furthermore, all methods converge very slowly

TABLE VI

The Error in the Calculation of the g.s. Energy of the Exponential Potential

| N. POINTS | 10 | 20 | 30 | 40 |
|---|---|---|---|---|
| PW | 1.1868 | 0.1140 | 0.0215 | 0.0066 |
| (1/0) | 0.7133 | -0.2841 | -0.1748 | -0.1040 |
| (2/0) | 1.0163 | 0.0284 | -0.0035 | -0.0024 |
| (3/0) | 1.1039 | 0.0843 | 0.0157 | 0.0052 |
| (4/0) | 1.1391 | 0.1006 | 0.0196 | 0.0062 |
| (1/1) | 1.0876 | 0.0710 | 0.0102 | 0.0027 |
| (1/2) | 1.1423 | 0.1004 | 0.0192 | 0.0061 |
| (1/3) | 1.1615 | 0.1079 | 0.0207 | 0.0065 |
| (2/2) | 1.1732 | 0.1111 | 0.0212 | 0.0065 |
| (3/3) | 1.1834 | 0.1135 | 0.0215 | 0.0066 |

*Note.* The exact value is $-6.7472$ and the quantity tabulated is $E_{\text{comp}} - E_{\text{exact}}$.

with $N_p$, and even with $N_p = 70$ the absolute error is still of order $10^{-4}$ for all methods. In our opinion the origin of this situation is the same as the origin of the particular behaviour of the odd angular momentum levels of the harmonic oscillator, and in the next section we shall point out a possible explanation.

When going to the continuum the situation changes: again the phase shifts determined with the PW method are the best ones, showing very good agreement with the theoretical results [10].

## 4. CONCLUSIONS AND COMMENTS

The examples studied in Section 3 permit us to establish the following results.

(1)   The PW method is the limiting case of subfamilies of matrix methods based in the finite-difference scheme.

(2)   The PW method is a simple and suitable method to compute both bound states and continuum phase shifts, giving very good results with a very small number of points.

(3)   Any knowledge of the properties of the potential or the solutions should be appropriately used to correctly state the numerical work, resulting in a considerable improvement of the results.

There still remain three important questions regarding our examples.

(1)   Why are odd partial waves of the harmonic oscillator so badly determined with respect to the even states?

(2)   Why does the exponential potential exhibit anomalous behaviour?

(3)   Why are the $[N/M]$ methods so inefficient for the determination of the phase shifts?

The answer to question 3 is very simple: the continuum states are mainly sensitive to the high energy states involved in the momentum representations. A look at Fig. 2 of I, which represents the kinetic energy contribution to the Hamiltonian matrix as given by the various integration methods, offers a straightforward answer to question 3: the increase of $N + M$ is more efficient in improving the low energy matrix elements than the high energy ones, so that all $[N/M]$ methods should break at the upper levels of the spectrum. For this reason, the corresponding phase shifts are completely wrong.

Neither of the other two questions has a simple answer. In our opinion the anomalous situation is a consequence of the properties of the related wave functions at short distances, their behaviour being incompatible with the particular periodic conditions hidden in our matrix formulation of the finite-difference integration methods. Let us consider the odd partial waves solutions of the harmonic oscillator: if the exact solutions are analytically continued to the negative $r$ region, then the odd waves will be symmetric around the origin, whereas the matrix formulation assumes
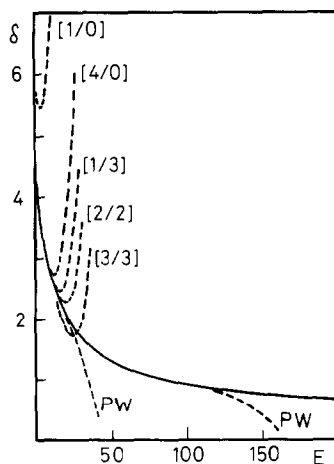
FIG. 2. Comparison of the exact phase shifts (—) with the computed values (– – –) for the exponential well. The phase shift is measured in radians. $R_{max} = 10$ and $N_p = 20$. The curve labelled PW extending up to 170 is computed with 40 points and with the same $R_{max}$.

an antisymmetric behaviour (remember that the reduced Schrödinger equation refers to the radial function divided by $r$, so that the symmetry properties are not the usual). In particular, the sine basis, $F_n = \sin nr$, at $r = 0$ spans the same Hilbert space as the polynomial basis $r, r^3, r^5,..., r^{2n-1}$, i.e., odd polynomials. It is certainly impossible to represent an even function in terms of odd polynomials, *unless both are null*, and this is what happens when the step goes to zero. The antisymmetry conditions only propagate to few columns of the Hamiltonian matrix, and if $h \to 0$ this propagation is harmless. In this form we understand why the convergence is so slow, and also why there is no breaking at all, i.e., we still have convergence. We also understand why this problem does not affect the Morse potential, the high barrier at short distances assuring that the wave function is negligibly small in that region. On the other hand, the solutions of the exponential potential do not have definite symmetry properties when extended to negative $r$ regions, and this explains the anomalous results of Table VI. Finally, the $s$-wave states of the harmonic oscillator and the Hylleraas potential are antisymmetric, and no problem arises.

The explanation suggests the convenience of generalizing the PW method by avoiding the antisymmetry requirements while maintaining the same description of the potential through the mere values on a given mesh.

### ACKNOWLEDGMENTS

## REFERENCES

1. R. GUARDIOLA AND J. ROS, *J. Comput. Phys.*, in press.
2. G. W. STEWART, *Comm. ACM* **13** (1970), 365.
3. E. A. HYLLERAAS, *Z. Phys.* **107** (1937), 258.
4. A. GALINDO AND P. PASCUAL, "Mecánica Cuantica," Alhambra, Madrid, 1970.
5. R. GUARDIOLA AND P. PASCUAL, *An. Fís.* **63** (1967), 279.
6. B. G. WICKE AND D. O. HARRIS, *J. Chem. Phys.* **64** (1976), 5236.
7. B. W. SHORE, *J. Chem. Phys.* **59** (1973), 6450.
8. P. M. MORSE, *Phys. Rev.* **34** (1929), 57.
9. D. J. LOCKER, *J. Phys. Chem.* **75** (1971), 1756.
10. R. GUARDIOLA, "Estudio Analítico de la Matriz *S*," Tesina Univ., Valencia, Spain, 1966.